IEEE Access
Multidisciplinary | Rapid Review | Open Access Journal

Received September 21, 2017, accepted October 7, 2017, date of publication October 12, 2017,
date of current version November 7, 2017.

Digital Object Identifier 10.1109/ACCESS.2017.2762361

Hybrid Beamforming Designs for Massive MIMO Millimeter-Wave Heterogeneous Systems

DANIEL CASTANHEIRA, PEDRO LOPES, ADÃO SILVA, AND ATÍLIO GAMEIRO
Instituto de Telecomunicações and DETI, University of Aveiro, 3810-193 Aveiro, Portugal

Corresponding author: Daniel Castanheira (dcastanheira@av.it.pt)

This work was supported in part by the National Funds through the Fundação para a Ciencia e a Tecnologia under the PURE-5GNET Project under Grant UID/EEA/50008/2013, in part by the European Structural and Investment Funds through the Competitiveness and Internationalization Operational Program—COMPETE 2020, and in part by the National Funds through the Foundation for Science and Technology under the Project RETIOT under Grant POCI-01-0145-FEDER-016432.

ABSTRACT Network densification through the deployment of small cells along the coverage area of a macro-cell, employing massive multiple input multiple output (MIMO) and millimeter-wave (mmWave) technologies, is a key approach to enhancing the network capacity and coverage of future systems. For ultra-dense mmWave heterogeneous scenarios with a massive number of users, one should address both inter- and intra-tier interferences contrary to the low-density scenarios, where the network is mainly noise limited. Therefore, this paper proposes low complex hybrid analog–digital receive and transmit beamforming techniques for ultra-dense uplink massive MIMO mmWave heterogeneous systems to efficiently mitigate these interferences. At the small cells, the hybrid analog–digital receive beamforming/equalizer is computed in a distributed fashion, where the analog processing is performed at the small cell base stations or access points and the digital part at a central unit for joint processing. To optimize the analog part of the hybrid equalizer and the precoders used at the user terminals, we consider as a metric the distance relative to the fully digital counterpart induced by the Frobenius norm. In the optimization problem, apart from the analog constraints usually considered in the homogeneous systems, we further impose the constraints inherent to the distributed nature of the access points. To cancel the inter-tier interference, the digital parts of the precoders employed at the small cell user terminals are designed so that this interference resides in a low-dimensional subspace at the macro base station. The results show that the performance of the proposed hybrid analog–digital precoder/equalizer scheme is close to the fully digital counterpart and is able to efficiently remove both inter- and intra-tier interferences.

INDEX TERMS Heterogeneous networks, massive MIMO, millimeter wave communications, hybrid analog/digital architectures.

I. INTRODUCTION

With the constant increase in mobile communication devices and services, the system requirements become more demanding. To satisfy some of these requirements, such as better coverage and higher data rates, mobile operators have been deploying small cells within the existing macro-cells. They operate inside the coverage area of a macro-cell, creating a heterogeneous network (HetNet), and offer great advantages for operators and for users, allowing better coverage and higher data rates [1]–[3]. However, heterogeneous networks are not sufficient to cope with these demands, so further technologies need to be researched and developed. Massive MIMO and millimeter wave (mmWave) are some of such technologies, which have proven to be solid choices to meet these demands [4]–[6].

Due to its frequency, several times greater than the current systems, mmWave has the potential to achieve multi-gigabit per second data rates [5]. However, the wireless propagation characteristics are quite different from the current sub-6 GHz band [7], [8], as it degrades with the increase in frequency because special care is needed when designing beamforming schemes [9]. In addition to mmWave, the deployment of a massive number of antennas has also been considered a key technology for meeting the ever-increasing demand for higher data rates in 5G or B5G networks [10]. Massive MIMO can scale up MIMO by orders of magnitude compared to the conventional MIMO systems [11]. A survey on massive MIMO, also known as large-scale MIMO, including channel modeling, applications scenarios and physical and networking techniques, was provided in [12].

There are some advantages of combining mmWave with massive MIMO since it allows packing a higher number of antennas into the same volume due to a small mmWave wavelength [13]. As a consequence, both terminals can be equipped with a massive number of antennas, which will allow designing efficient beamforming techniques that can compensate for the attenuation from higher frequencies. However, the design of these beamforming techniques should follow different approaches than the approaches adopted for lower frequency counterparts, mainly due to the hardware limitations [14]. In fact, the high cost and power consumption of some mmWave mixed-signal components make it difficult to have a fully dedicated radio frequency (RF) chain for each antenna [15] as in conventional MIMO systems, so the design of full digital beamforming approaches is not realistic for massive MIMO mmWave-based systems. The simplest solution for the number of RF chains is the use of full analog beamforming with phase shifters [14], but it employs only a quantized number of phase shifts and their constraints on the amplitudes, which leads to a limitation on the system performance, as discussed in [16]. To tackle these limitations, hybrid analog-digital beamforming approaches, where some signal processing is done at the digital level and some left to the analog domain, have been discussed in [17]–[22]. A hybrid analog-digital spatially sparse transmit and receive beamforming scheme was proposed in [17]. The spatial structure of mmWave channels was considered to formulate the beamforming scheme as a sparse reconstruction problem. In [18], a multi-user receive beamforming was designed to efficiently address the multi-user interference caused by the single antenna user terminals sharing the same spectrum. In [19], a hybrid beamforming algorithm was proposed for the downlink assuming limited feedback channel information. An efficient hybrid iterative block space-time multi-user equalizer has been proposed [20]. Hybrid precoding solutions and codebook design for limited feedback wideband mmWave systems were discussed in [21]. To flatten the fading channel over a wide band and maximize the system capacity, a signal-to-interference ratio constrained capacity maximization algorithm to jointly design the precoder and the combiner was derived in [22]. In [23] an iterative matrix decomposition based hybrid beamforming scheme for a single-user scenario and a novel subspace projection based angle of arrival aided block diagonalization for downlink multiuser scenario have been proposed. The authors in [24] designed hybrid RF and baseband precoders/combiners for multistream transmission in massive MIMO mmWave systems, by directly decomposing the predesigned unconstrained digital precoder/combiner of a large dimension. In [25] the authors proposed a novel iterative algorithm for the joint hybrid precoder and combiner design by exploiting the duality of the uplink and downlink MU-MIMO channels.

The prior works were focused primarily on hybrid digital-analog beamforming approaches for homogeneous systems, i.e., only a single cell is assumed. In fact, most of the work done in the last years for heterogeneous systems assumed a sub-6 GHz band [26]. In the HetNets, considering that the small cells coexist under the same spectrum with the macro-cell (approach followed in this paper), the levels of interference are too high. Evidently, this requires the development of efficient interference management schemes, since, if not carefully designed, the small cells signals may cause interference on the macro-cell [1]. Interference alignment [27], [28] is an effective approach to address interference in the two-tiered networks [29]–[34]. A technique that takes advantage of the orthogonal frequency division multiplexing (OFDM) cyclic prefix for IA was proposed in [29]. The work in [30] studied several IA approaches with different levels of inter-system information sharing. The problem of IA, pre-coded under limited information exchange, for narrowband heterogeneous based networks, was analytically approached in [31]. The authors in [32] combined IA with an iterative block decision feedback equalization (IB-DFE) [33] principle to remove the inter-tier interference for the uplink SC-FDMA systems. Another efficient approach to cancel the interference generated from small cells at the macro-cell user terminal is the application of joint signal alignment (SA) and physical network coding (PNC) as discussed in [34] and [35]. As noted in [36], the use of mmWave and massive MIMO in the context of heterogeneous networks would be a key factor to increase the network capacity for future 5G networks. For a low dense scenario and due to the short range of mmWave communications, it is expected that the users on a given small cell would not interfere with other small cells and macro cells, and the system is mainly noise-limited. However, in ultra-dense scenarios with a massive number of users the system becomes interference-limited, even using the mmWave band [37] since at the mmWave band, the channel shows significant differences for line-of-sight (LOS) and non-line-of-sight (NLOS) path loss characteristics. For example, channel measurements show a path loss exponent of approximately 2 for LOS and an exponent as large as 5.76 in downtown New York City [38]. As shown in [37], when the density of the network is very high (for example, in ultra-dense networks) the interference is significant since for ultra-dense scenarios, a user sees several LOS base stations and thus experiences significant interference. As mentioned in [37], the development of more advanced interference management techniques is an interesting topic for ultra-dense massive MIMO mmWave-based networks.

In this paper, we report the design of low complex hybrid analog-digital transmit and receive beamforming (or precoder/equalizer) for ultra-dense uplink massive MIMO mmWave HetNets networks. To the best of our knowledge, uplink hybrid beamforming approaches designed for massive MIMO mmWave in the context of HetNets has not been addressed in the literature. The main contributions of this work include:

- At the small cells, we assume a distributed hybrid analog-digital architecture, where the analog part is performed at the small cell base stations and the digital part at the central unit for joint processing. The main

motivation to consider a distributed hybrid analog-digital processing at the small cells is that the information to be sent by the access points to the central unit is significantly reduced since the number of RF chains is much lower than the number of antennas. Moreover, the signals are transported through the front-haul in the analog domain.

- To efficiently cancel the inter-tier interference, the digital part of the precoders employed at the small cells user terminals are designed so that this interference resides in a low dimension at the macro base station. We show numerically that 2 bits of inter-tier information exchange are enough to efficiently align the inter-tier interference with a good overall network performance.
- To optimize the analog part of the hybrid equalizer and the precoders used at both the macro and small cell user terminals, we minimize the distance between the hybrid and the fully digital approaches. In the optimization problem, we impose the constraints of the analog part and the constraints inherent to the distributed nature of the small cells access points. This approach is significantly different from the single tier case where the analog and digital parts are centralized and therefore, the optimization problem is less complex.

Notations: Boldface capital letters denote matrices and boldface lowercase letters denote column vectors. The operations $(.)^T$, $(.)^H$, $(.)^*$ and $tr(.)$ represent the transpose, the Hermitian transpose, the conjugate and the trace of a matrix. The operator sign(a) represents the sign of the real number a. For a complex number c, $\text{sign}(c) = \text{sign}(\Re(c)) + j\text{sign}(\Im(c))$, where $\Re(c)(\Im(c))$ represents the real part of c (imaginary part of c). The operator sign(.) is applied element-wise to matrices. Consider a vector $\mathbf{a}$ and a matrix $\mathbf{A}$, then diag($\mathbf{a}$) and diag($\mathbf{A}$) correspond to a diagonal matrix with diagonal entries equal to vector $\mathbf{a}$ and a diagonal matrix with entries equal to the diagonal entries of the matrix $\mathbf{A}$, respectively. $\mathbf{A}(j, l)$ denotes the element at row j and column l of the matrix $\mathbf{A}$. $\mathbf{I}_N$ is the identity matrix with size $N \times N$. The index u refers to the user terminal and p the receiver.

II. SYSTEM MODEL

We consider the uplink of a two-tiered network whose carrier frequency is in the mmWave band. The two-tiered network comprises a macro-cell with N small cells within its coverage area (all sharing the same frequency spectrum), as depicted in Fig. 1. The macro-cell has a base station (BS) and one user terminal (UT). Each small cell has an access point (AP) which serves the UT. The APs have an analog-only architecture, i.e., the signals are processed in the analog domain. The processed analog domain signals are sent through a fiber-based front-haul network to a central unit (CU), where they are digitized and jointly processed in the digital domain. Namely, for the small cells, the analog and digital processing are distributed (the analog processing is done at the APs and the digital processing at the CU) and for the macro-cell, the analog-digital processing is centralized at the BS.

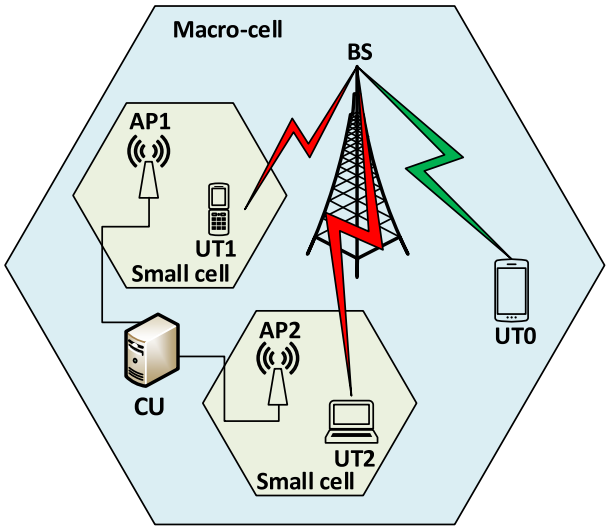

FIGURE 1. System model, example with 2 small cells within the macro-cell.

At the receiver side, the small cells have two entities, the N APs, which perform the analog processing and a CU which performs the digital processing. In contrast, the macro-cell has just one entity, the BS, which performs both the analog and digital processing. To simplify the description, in the following sections we divide the BS into two logical entities, equivalent to the ones at the small cells, where the analog and digital processing occurs. With a slight abuse of terminology, we will denominate by BS the logical entity performing the digital processing and will give a different name to the analog entity. Henceforth, to uniformize the notation between the macro and small cells, the macro UT is denoted by UT_0 and the UT of the p^{th} small cell by UT_p. At the receiver side, the logical entity that performs the analog processing is denoted by RX_p, with $p \in \{0, \ldots, N\}$. The digital domain entities are denoted by BS and CU, for the macro and small cells, respectively. From now on, we assume that the UT_p and RX_p have L_p and M_p antennas, respectively.

For this work, we consider the uplink direction, where each UT transmits N_s data streams to its respective receiver. The received signal at RX_p is given by

$$\mathbf{y}_p = \sum_{u=0}^{N} \mathbf{H}_{p,u}\mathbf{x}_u + \mathbf{n}_p, \tag{1}$$

where $\mathbf{y}_p \in \mathbb{C}^{M_p}$ denotes the received signal, $\mathbf{x}_u \in \mathbb{C}^{L_u}$ the UT_u transmitted signal, $\mathbf{n}_p \in \mathbb{C}^{M_p}$ the white Gaussian noise with variance σ^2 and $\mathbf{H}_{p,u} \in \mathbb{C}^{M_p \times L_u}$ the channel between UT_u and RX_p.

A. USER TERMINAL ARCHITECTURE

For UT_u a hybrid analog-digital architecture, as depicted in Fig. 2, is considered. In this architecture, UT_u is equipped with T_u transmitting RF chains. As such, the transmitted

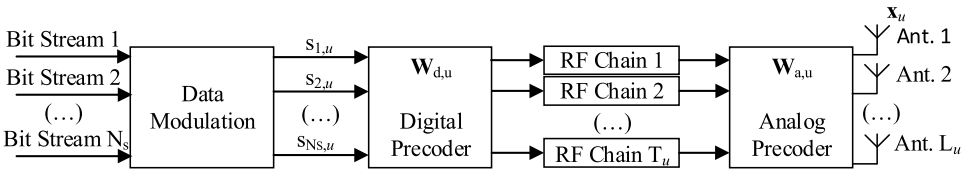

FIGURE 2. User terminal block diagram.

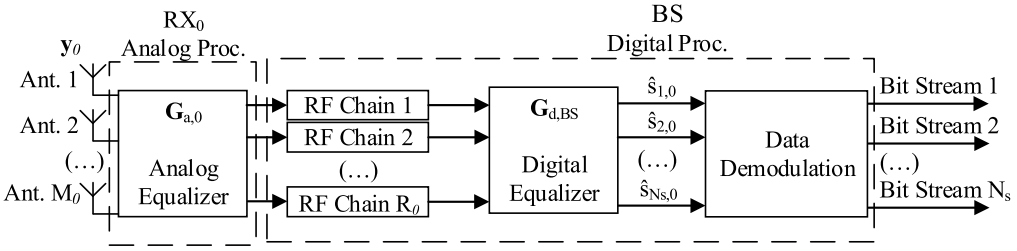

FIGURE 3. Block diagram of the macro-cell receiver.

signal is given by

$$\mathbf{x}_u = \mathbf{W}_{a,u}\mathbf{W}_{d,u}\mathbf{s}_u, \tag{2}$$

where $\mathbf{W}_{a,u} \in \mathbb{C}^{L_u \times T_u}$ is the analog precoder, which is comprised of a number of phase-shifters that connect each RF chain to all transmit antennas, $\mathbf{W}_{d,u} \in \mathbb{C}^{T_u \times N_s}$ the digital precoder and $\mathbf{s}_u \in \mathbb{C}^{N_s}$ denotes the UT$_u$ data symbols modulated using an M-QAM constellation. The precoders must be designed such that the power constraint $\left\|\mathbf{W}_{a,u}\mathbf{W}_{d,u}\right\|_F^2 = N_s$ is respected.

B. RECEIVER ARCHITECTURE

As previously mentioned, at the receiver side, the analog processing is performed at RX$_p$ and the digital processing at the BS or CU. In the following sections, we will describe the analog and digital processing in two different sections.

1) ANALOG DOMAIN

As previously mentioned at RX$_p$, we consider an analog only architecture (see Fig. 3 and Fig. 4). The RX$_p$ has M_p antennas and outputs R_p signals to the digital processing entity. RX$_p$ performs a linear map between its inputs and outputs. This mapping may be mathematically described by

$$\hat{\mathbf{s}}_{a,p} = \mathbf{G}_{a,p}^H \mathbf{y}_p, \tag{3}$$

where $\hat{\mathbf{s}}_{a,p} \in \mathbb{C}^{R_p}$ denotes the vector containing the R_p outputs of RX$_p$ and $\mathbf{G}_{a,p} \in \mathbb{C}^{M_p \times R_p}$ the analog equalizer, which is comprised of a number of phase-shifters that connect each output to all receiving antennas.

2) DIGITAL DOMAIN

For the digital domain processing, we will just describe the model for the CU, since for the BS, the description is identical to the case where the CU processes only one small cell ($N = 1$). The CU receives the signal $\hat{\mathbf{s}}_{a,CU} = [\hat{\mathbf{s}}_{a,1}^T, \ldots, \hat{\mathbf{s}}_{a,N}^T]^T \in \mathbb{C}^{R_1+\ldots+R_N}$ through the front-haul. This signal is first digitized by $R_{CU} = R_1 + \ldots + R_N$ RF chains and then processed by the digital equalizer at baseband frequency. The estimated symbols at the CU are given by

$$\hat{\mathbf{s}}_{d,CU} = \mathbf{G}_{d,CU}^H \hat{\mathbf{s}}_{a,CU}, \tag{4}$$

where $\hat{\mathbf{s}}_{d,CU} = [\hat{\mathbf{s}}_0^T, \ldots, \hat{\mathbf{s}}_u^T, \ldots, \hat{\mathbf{s}}_N^T]^T$ denotes the estimated transmitted symbols from each UT, with $\hat{\mathbf{s}}_u \in \mathbb{C}^{N_s}$ and $\mathbf{G}_{d,CU} \in \mathbb{C}^{R_{CU} \times (N+1)N_s}$ is the digital equalizer. One of the dimensions of the digital part of the equalizer is equal to the total number of streams sent by the $N+1$ UTs. Therefore, one requirement for resolvability of all streams is $R_{CU} \geq (N+1)N_s$.

C. CHANNEL MODEL

For the channel model, a narrowband clustered channel based on the Saleh-Valenzuela is adopted. As discussed in [9], the channel $\mathbf{H}_{p,u}$, $p, u \in \{0, \ldots, N\}$ is considered the sum of the contributions of N_{cl} scattering clusters, where each of the clusters contributes N_{ray} propagation paths to the channel matrix $\mathbf{H}_{p,u}$. The matrix channel $\mathbf{H}_{p,u}$ can be described by

$$\mathbf{H}_{p,u} = \gamma \sum_{i,l} \alpha_{il}^{p,u} \mathbf{a}_{p,u}(\phi_{il}^{p,u}, \theta_{il}^{p,u}) \mathbf{b}_{p,u}(\varphi_{il}^{p,u}, \vartheta_{il}^{p,u})^*, \tag{5}$$

where $\gamma = \sqrt{N_t N_r / N_{cl} N_{ray}}$ denotes the normalization factor; $\alpha_{il}^{p,u}$ the complex gain of the *i-th* scattering cluster and the l^{th} ray for the channel between UT$_u$ and RX$_p$, where both $\phi_{il}^{p,u}(\theta_{il}^{p,u})$ and $\varphi_{il}^{p,u}(\vartheta_{il}^{p,u})$ represent its azimuth (elevation) angles of arrival and departure for the link between RX$_p$ and UT$_u$ respectively; $\mathbf{a}_{p,u}$ ($\mathbf{b}_{p,u}$) the normalized receive (transmit) array response for the link between RX$_p$ and UT$_u$. In the following, we will also use the matrix form of (5)

$$\mathbf{H}_{p,u} = \mathbf{A}_{p,u}\mathbf{\Lambda}_{p,u}\mathbf{B}_{p,u}^H, \tag{6}$$

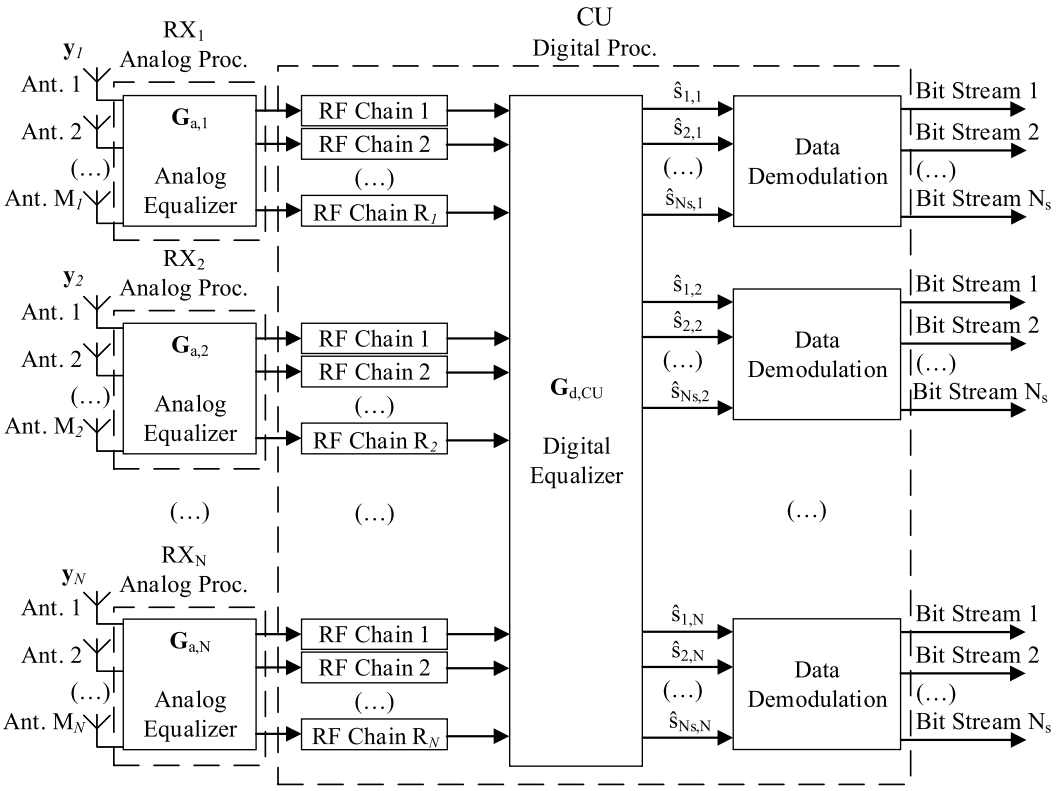

FIGURE 4. Central unit block diagram.

where $\mathbf{\Lambda}_{p,u}$ is a diagonal matrix where the entries are given by

$$\{\gamma\alpha_{il}^{p.u}\}_{1\leq i\leq N_{cl},1\leq l\leq N_{ray}},$$

$$\mathbf{A}_{p,u}=[\mathbf{a}_{p,u}(\phi_{il}^{p,u},\theta_{il}^{p,u})]_{1\leq i\leq N_{cl},1\leq l\leq N_{ray}}$$

and $\mathbf{B}_{p,u}=[\mathbf{b}_{p,u}(\varphi_{il}^{p,u},\vartheta_{il}^{p,u})]_{1\leq i\leq N_{cl},1\leq l\leq N_{ray}}$.

III. HYBRID PRECODER AND EQUALIZER DESIGN

In massive MIMO mmWave systems, the implementation of full digital algorithms can be impractical, as each antenna requires a dedicated RF chain. Hybrid designs are taken into consideration at both the transmitter and receiver terminals in this work. For the sake of simplicity and without loss of generality, in this section we describe only the design of the small cell precoder and equalizer, since the macro-cell precoder and equalizer may be obtained using a similar approach. For the macro BS, the N small cell UTs may be considered as just one UT, since we use interference alignment to align the signals of these N terminals at the BS.

A decoupled design is considered. First, we design the analog part, and then with the knowledge of the analog part, we design the digital part. Apart from simplifying the design of the analog and digital parts, this decoupled procedure brings further benefits. Namely, the channel between UT_u and RX_0 has dimensionality L_uM_0. By including the analog precoder and equalizer at both ends of the channel, the resulting equivalent channel has dimensionality T_uR_0. As the number of RF chains is much smaller than the number of antennas, then the dimensionality of the equivalent channel is much smaller than the dimensionality of the original channel. This fact significantly reduces the overhead necessary to estimate such channels, a factor that will be important in the design of the digital precoder of the small cell UTs which requires the knowledge of the inter-tier channels and uses the interference alignment technique to align the inter-tier interference along a low dimensional subspace.

A. ANALOG EQUALIZER AND PRECODER DESIGN

For the analog part, we propose two types of equalizers/precoders, one that is randomly generated and another that considers the channel information and the specific characteristics of mmWave-channels (specifically the sparsity) to compute the analog precoder.

In the following, we just describe the analog equalizer design, since the analog precoder is similar. The main difference between the two is the value of the weighting matrix $\mathbf{R}$ in the optimization problem (11). For the precoder, this matrix is equal to the identity but for the equalizer, it corresponds to the received signal correlation matrix.

1) RANDOM EQUALIZER

In random design, the analog decoder is randomly generated. By doing this, the receiver does not need information about the channel, simplifying the overall system design and

reducing the overhead required to estimate the channel. As the analog part is composed of a matrix of analog phase shifters, each element of the decoder must be normalized, so that ($|\mathbf{G}_{a,p}(i,j)|^2 = M_p^{-1}$). The analog equalizer may then be expressed as

$$\mathbf{G}_{a,p} = e^{i2\pi\boldsymbol{\Theta}_p}, \tag{7}$$

where $\boldsymbol{\Theta}_p \in \mathbb{C}^{M_p \times R_p}$ denotes a matrix of uniform random numbers, such that $\boldsymbol{\Theta}_p(i,j) \in [0,1]$, with $i \in \{1,\ldots,M_p\}$ and $j \in \{1,\ldots,R_p\}$ and the exponential is applied element-wise to the matrix $\boldsymbol{\Theta}_p$.

2) PROPOSED DISTRIBUTED HYBRID EQUALIZER FOR HETEROGENEOUS NETWORKS

From (3) and (4), it follows that the equalized signal at the CU is given by

$$\hat{\mathbf{s}}_{d,CU} = \mathbf{G}_{d,CU}^H \mathbf{G}_{a,CU}^H \mathbf{y}_{CU}, \tag{8}$$

where $\mathbf{G}_{a,CU} = \text{diag}(\mathbf{G}_{a,1},\ldots,\mathbf{G}_{a,N})$ and $\mathbf{y}_{CU} = [\mathbf{y}_1^T,\ldots,\mathbf{y}_N^T]^T$. By (1), (2) follows that

$$\hat{\mathbf{s}}_{d,CU} = \mathbf{G}_{d,CU}^H \mathbf{G}_{a,CU}^H \mathbf{H}_{CU}\mathbf{W}\mathbf{s} + \mathbf{G}_{d,CU}^H \mathbf{G}_{a,CU}^H \mathbf{n}_{CU} \tag{9}$$

where $\mathbf{H}_{CU} = [\mathbf{H}_{p,u}]_{1\le p\le N, 0\le u\le N}$, $\mathbf{W} = \text{diag}(\mathbf{W}_{a,u}\mathbf{W}_{d,u})_{0\le u\le N}$, $\mathbf{s}=[\mathbf{s}_u]_{0\le u\le N}$ and $\mathbf{n}_{CU} = [\mathbf{n}_p]_{0\le p\le N}$.

Let $\mathbf{G}_{CU,opt}$ denote the optimum fully digital equalizer. If we use as a metric the mean square error, then the optimum fully digital equalizer is the Minimum Mean Square Error (MMSE) which is given by

$$\mathbf{G}_{CU,opt} = \left(\mathbf{W}^H\mathbf{H}_{CU}^H\mathbf{H}_{CU}\mathbf{W} + \sigma^2\mathbf{I}_{N_s}\right)^{-1}\mathbf{W}^H\mathbf{H}_{CU}^H \tag{10}$$

To optimize the analog part of the equalizer, we will use as a metric the weighted Frobenius norm [17] between the fully digital and hybrid equalizers. Mathematically, this corresponds to

$$\mathbf{G}_{a,CU} = \arg\min \left\|\mathbf{R}^{1/2}\left(\mathbf{G}_{CU,opt} - \mathbf{G}_{a,CU}\mathbf{G}_{d,CU}^{opt}\right)\right\|_F^2 \quad s.t.\ \mathbf{G}_{a,CU} \in \mathcal{G}_a. \tag{11}$$

where $\mathbf{R} = \mathbf{H}_{CU}\mathbf{W}\mathbf{W}^H\mathbf{H}_{CU}^H + \sigma^2\mathbf{I}$ denotes the correlation matrix [17] of the signal $\mathbf{y}_{CU} = [\mathbf{y}_p]_{1\le p\le N}$, and $\mathcal{G}_a$ denotes the set of all block-diagonal matrices with block-diagonal entries respecting the analog constraint ($|\mathbf{G}_{a,p}(i,j)|^2 = M_p^{-1}$). More specifically, the set $\mathcal{G}_a$ is given by $\mathcal{G}_a = \{\mathbf{G}_{a,CU} : \mathbf{G}_{a,CU} = \text{diag}(\mathbf{G}_{a,p})_{1\le p\le N}, |\mathbf{G}_{a,p}(i,j)|^2 = M_p^{-1}, \forall p \in \{1,\ldots,N\}\}$. In this optimization problem, we considered the optimum digital part to obtain the analog part of the equalizer, which accordingly to the KKT conditions is given by

$$\mathbf{G}_{d,CU}^{opt} = \left(\mathbf{G}_{a,CU}^H\mathbf{R}\mathbf{G}_{a,CU}\right)^{-1}\mathbf{G}_{a,CU}^H\mathbf{R}\mathbf{G}_{CU,opt}. \tag{12}$$

Using (12), the optimization problem simplifies to

$$\mathbf{G}_{a,CU} = \arg\min \left\|\mathbf{Q}\mathbf{R}^{1/2}\mathbf{G}_{CU,opt}\right\|_F^2 \quad s.t.\ \mathbf{G}_{a,CU} \in \mathcal{G}_a. \tag{13}$$

where $\mathbf{Q} = \mathbf{I} - \mathbf{R}^{1/2}\mathbf{G}_{a,CU}\left(\mathbf{G}_{a,CU}^H\mathbf{R}\mathbf{G}_{a,CU}\right)^{-1}\mathbf{G}_{a,CU}^H\mathbf{R}^{H/2}$. By expanding the merit function of the optimization problem (13), we verify that it is equal to a constant minus a term that is dependent on $\mathbf{G}_{a,CU}$. Therefore, (13) simplifies to

$$\mathbf{G}_{a,CU} = \arg\max \left\|\left(\mathbf{G}_{a,CU}^H\mathbf{R}\mathbf{G}_{a,CU}\right)^{-1/2}\mathbf{G}_{a,CU}^H\mathbf{R}\mathbf{G}_{CU,opt}\right\|_F^2 \quad s.t.\ \mathbf{G}_{a,CU} \in \mathcal{G}_a. \tag{14}$$

To solve (14), we propose to iteratively optimize the analog equalizer matrix column by column. Let $\mathbf{G}_{a,CU}^{(i-1)}$ denote the output of the optimization problem at iteration $i-1$ and $\mathbf{G}_{a,CU}^{(i)} = [\mathbf{G}_{a,CU}^{(i-1)}, \mathbf{g}_{a,CU}^{(i)}]$ where $\mathbf{g}_{a,CU}^{(i)}$ denotes the column we are optimizing at the iteration i, then using the Gram-Schmidt orthogonalization follows that $\mathbf{R}^{1/2}\mathbf{G}_{a,CU}^{(i)}((\mathbf{G}_{a,CU}^{(i)})^H\mathbf{R}\mathbf{G}_{a,CU}^{(i)})^{-1/2}, = [\mathbf{U}^{(i-1)}, \mathbf{P}^{(i-1)}\mathbf{R}^{1/2}\mathbf{g}_{a,CU}^{(i)}]$ with $\mathbf{P}^{(i-1)} = \mathbf{I} - \mathbf{U}^{(i-1)}\mathbf{U}^{(i-1)^H}$ and $\mathbf{U}^{(i-1)} = \mathbf{R}^{1/2}\mathbf{G}_{a,CU}^{(i-1)}((\mathbf{G}_{a,CU}^{(i-1)})^H\mathbf{R}\mathbf{G}_{a,CU}^{(i-1)})^{-1/2}$. Therefore, the objective at iteration i is to find column i of the analog equalizer, which is given by

$$\mathbf{g}_{a,CU}^{(i)} = \arg\max \mathbf{G}_{CU,opt}^H\mathbf{R}^{H/2}(\mathbf{U}^{(i-1)}\mathbf{U}^{(i-1)^H} + \mathbf{P}^{(i-1)}\mathbf{R}^{1/2}\mathbf{g}_{a,CU}^{(i)}(\mathbf{g}_{a,CU}^{(i)})^H\mathbf{R}^{H/2}\mathbf{P}^{(i-1)})\mathbf{R}^{1/2}\mathbf{G}_{CU,opt} \quad s.t.\ \mathbf{g}_{a,CU}^{(i)} \in \mathcal{G}_a. \tag{15}$$

and equivalent to

$$\mathbf{g}_{a,CU}^{(i)} = \arg\max \left\|\mathbf{C}^{(i-1)}\mathbf{g}_{a,CU}^{(i)}\right\|^2 \quad s.t.\ \mathbf{g}_{a,CU}^{(i)} \in \mathcal{G}_a. \tag{16}$$

where $\mathbf{R}^{(i-1)} = \mathbf{R}^{H/2}\mathbf{P}^{(i-1)}\mathbf{R}^{1/2}$ and $\mathbf{C}^{(i-1)} = \mathbf{G}_{CU,opt}^H\mathbf{R}^{(i-1)}$. Accordingly, to the definition of the constraint set $\mathcal{G}_a$, the optimum analog equalizer must have a block diagonal structure. Let us decompose matrix $\mathbf{C}^{(i-1)}$ in N blocks along its columns, i.e., $\mathbf{C}^{(i-1)} = [\mathbf{C}_1^{(i-1)},\ldots,\mathbf{C}_p^{(i-1)},\ldots,\mathbf{C}_N^{(i-1)}]$. Then, by including the block diagonal constraint in the merit function of the optimization problem (16) follows

$$(\mathbf{g}_{a,p}^{(i)}, p) = \arg\max \left(\max_p \left\{\left\|\mathbf{C}_p^{(i-1)}\mathbf{g}_{a,p}^{(i)}\right\|^2\right\}\right) \quad s.t.\ \mathbf{g}_{a,p}^{(i)} \in \bar{\mathcal{G}}_a, \quad \forall p \in 1,\ldots,N \tag{17}$$

where $\mathbf{g}_{a,p}^{(i)}$ denotes a column of the analog part of the equalizer of RX_p, and $\bar{\mathcal{G}}_a = \{\mathbf{g}_{a,p} : |\mathbf{g}_{a,p}(i)|^2 = M_p^{-1}\}$. To solve (17), we find the optimum value of $\mathbf{g}_{a,p}^{(i)}$ for all $p \in \{1,\ldots,N\}$ and then select the index p that corresponds to the maximum among all $p \in \{1,\ldots,N\}$. For RX_p this corresponds to

$$\mathbf{g}_{a,p}^{(i)} = \arg\max \left\|\mathbf{C}_p^{(i-1)}\mathbf{g}_{a,p}^{(i)}\right\|^2, \quad s.t.\ \mathbf{g}_{a,p}^{(i)} \in \bar{\mathcal{G}}_a \tag{18}$$

If we replace the constraint $|\mathbf{g}_{a,p}(i)|^2 = M_p^{-1}$ with the relaxed constraint $||\mathbf{g}_{a,p}||^2 = 1$, then the optimum value of the previous problem is equal to the maximum eigenvalue of the positive-semidefinite matrix $(\mathbf{C}_p^{(i-1)})^H\mathbf{C}_p^{(i-1)}$, and $\mathbf{g}_{a,p}^{(i)}$ would be equal to the corresponding eigenvector. Therefore, a simple approach to ensure that the constraint $\mathbf{g}_{a,p}^{(i)} \in \bar{\mathcal{G}}_a$ is respected is to project the corresponding eigenvector along the set of vectors in the set $\mathbf{g}_{a,p}^{(i)} \in \bar{\mathcal{G}}_a$, which amounts to retaining the phase of each element of the optimum eigenvector and setting its magnitude to M_p^{-1}. A different approach to solve (18) would be to use a dictionary whose elements respect the constraint $\mathbf{g}_{a,p}^{(i)} \in \bar{\mathcal{G}}_a$ and select the best element from the dictionary as the optimum analog equalizer. Let us denote by $\mathcal{D}_p$ the dictionary used for RX_p. Therefore, the optimization problem corresponds to

$$\mathbf{g}_{a,p}^{(i)} = \arg \max_j \left\| \mathbf{C}_p^{(i-1)}\mathbf{g}_{a,p}^j \right\|^2 \tag{19}$$

where $\mathbf{g}_{a,p}^j$ denotes the element j of the dictionary $\mathcal{D}_p$. For the dictionary, we may use the array response matrix of RX_p, i.e., matrix $\mathbf{A}_p = [\mathbf{A}_{p,u}]_{0\le u\le N}$. From the definition of matrix $\mathbf{C}_p^{(i-1)}$, its row space is identical to the column space of the channel matrix $\mathbf{H}_{CU}$. Therefore, a similar conclusion applies for matrices $\mathbf{C}_p^{(i-1)}$ and $\mathbf{H}_p = [\mathbf{H}_{p,u}]_{0\le u\le N}$ (see definition of the channel matrix ($\mathbf{H}_{CU} = [\mathbf{H}_{p,u}]_{1\le p\le N, 0\le u\le N}$)). Hence, from (6), it follows that matrix $\mathbf{A}_p$ forms a good basis for the channel [17].

With the dictionary-based approach, the CU computes the analog equalizer for the N APs and then forwards to the APs the index of the R_p selected dictionary entries, or equivalently, forwards to RX_p the selected angles of arrival. In contrast, for the projection-based approach, the CU must forward to each RX_p, $p \in \{1,\ldots,N\}$ the full analog equalizer matrix $G_{a,p} \in \mathbb{C}^{R_p\times M_p}$ that corresponds to $R_p \times M_p$ real numbers. Due to its lower overhead, the dictionary-based approach is superior and is the one we will use to obtain the numerical results in Section V.

The pseudo-code for the proposed algorithm is given in Algorithm 1.

B. DIGITAL EQUALIZER DESIGN

For the digital part of the equalizer, we use the optimum digital equalizer as in equation (12), which we repeat here for completeness.

$$\mathbf{G}_{d,CU}^{opt} = \left(\mathbf{G}_{a,CU}^H\mathbf{R}\mathbf{G}_{a,CU}\right)^{-1}\mathbf{G}_{a,CU}^H\mathbf{R}\mathbf{G}_{CU,opt}. \tag{12}$$

As previously mentioned, the analog precoder and equalizer may be designed using similar procedures, since one may be considered as a specific case of the other. In contrast, the digital parts of the hybrid precoder and equalizer perform different functions. The digital part of the equalizer separates the received data signal into data streams, and the digital part of the precoder aligns the inter-tier interference along a small dimension subspace. In the next section, we describe the digital precoder.

Algorithm 1 The Proposed Hybrid Multi-User Linear Equalizer Algorithm for HetNets

Inputs: $\mathbf{G}_{CU,opt}$, $\mathbf{R}^{1/2}$

$\mathbf{P}^{(0)} = \mathbf{I}$
for $i = 1 : \text{R}_{CU}$
  $\mathbf{R}^{(i-1)} = \mathbf{R}^{H/2}\mathbf{P}^{(i-1)}\mathbf{R}^{1/2}$
  $\mathbf{C}^{(i-1)} = \mathbf{G}_{CU,opt}^H\mathbf{R}^{(i-1)}$
  for $q = 1 : N$
    $\mathbf{\Psi}_q = \mathbf{C}_q^{(i-1)}\mathbf{A}_q$
    $k_q = \arg\max_{l=1,\ldots,N_{cl}N_{ray}}(\mathbf{\Psi}_q^H\mathbf{\Psi}_q)_{\ell,\ell}$
  end for
  $p = \arg\max_{q=1,\ldots,N}(\mathbf{\Psi}_q^H\mathbf{\Psi}_q)_{k_q,k_q}$
  $\mathbf{G}_{a,p} = [\mathbf{G}_{a,p}, \mathbf{A}_p^{(k_p)}]$
  $\mathbf{G}_{a,\text{CU}} = [\mathbf{G}_{a,\text{CU}}, \mathbf{A}_p^{(k_p)}]$
  $\mathbf{U}^{(i-1)} = \mathbf{R}^{1/2}\mathbf{G}_{a,\text{CU}}^{(i-1)}((\mathbf{G}_{a,\text{CU}}^{(i-1)})^H\mathbf{R}\mathbf{G}_{a,\text{CU}}^{(i-1)})^{-1/2}$
  $\mathbf{P}^{(i-1)} = \mathbf{I} - \mathbf{U}^{(i-1)}\mathbf{U}^{(i-1)^H}$
end for
return : $\mathbf{G}_{a,\text{CU}}, \mathbf{G}_{a,1}, \ldots, \mathbf{G}_{a,N}$

C. DIGITAL PRECODER DESIGN

As discussed before for ultra-dense mmWave heterogeneous systems, the inter-tier interference from the small cell UTs to the macro-cell BS impacts the network performance. Therefore, our objective is to design the digital precoders of the small cell UTs so that the inter-tier interference is removed. To enforce the zero-interference condition, the following constraint must be respected.

$$\mathbf{G}_{d,0}^H\mathbf{F}_{0,u}\mathbf{W}_{d,u} = 0, \tag{20}$$

where $\mathbf{F}_{0,u} = \mathbf{G}_{a,0}^H\mathbf{H}_{0,u}\mathbf{W}_{a,u}$ denotes the equivalent channel between the BS and UT_u, considering both analog precoder and equalizer, which dimensionality is much smaller than the one of the original channel $\mathbf{H}_{0,u}$. Let us define matrix $\mathbf{V} = \text{null}(\mathbf{G}_{d,0})$. Then, from (20) it follows that

$$\mathbf{F}_{0,u}\mathbf{W}_{d,u} = \mathbf{V}, \tag{21}$$

The space spanned by the equivalent channel, including the digital precoder, i.e., channel $\mathbf{F}_{0,u}\mathbf{W}_{d,u}$, is identical across all small cell user terminals and equal to $\mathbf{V} \in \mathbb{C}^{R_0\times N_s}$, which we denominate by alignment direction. Therefore, the solution to the zero-interference condition is

$$\mathbf{W}_{d,u} = \text{null}(\mathbf{G}_{d,0}^H\mathbf{F}_{0,u}), \tag{22}$$

$$\mathbf{V} = \text{null}(\mathbf{G}_{d,0}), \tag{23}$$

According to the previous derivation, the alignment direction $\mathbf{V}$ completely defines the subspace where the full inter-tier interference resides. This subspace occupies a subspace with dimensionality N_s. In contrast, if condition (20) is not respected, the interference subspace dimensionality would be NN_s, i.e., N times higher. Furthermore, from (23), we verify that the alignment direction is a function of the BS digital equalizer and vice-versa. As the UT_u, $u \in \{1,\ldots,N\}$ precoder is a function of the digital equalizer of the BS

TABLE 1. Parameters for the two different scenarios.

Parameters	N_s	N	M_p	M_s	L_p	L_s	T_p	T_s	R_p	R_s
Scenario 1	1	2	32	16	16	16	1	2	2	2
Scenario 2	2	2	32	16	16	16	2	4	4	4

(or equivalently, of the alignment direction), this matrix must be known at all UTs. Several approaches may be considered to select the value of this matrix. In the following subsections, we describe three approaches in more detail. We assume that this matrix is selected at the macro BS, since its value will influence the performance of the macro-cell, and then it is forwarded to the small cells through the air. We start with the optimum approach, with the highest requirements in terms of information exchange between the macro and small cells and then proceed until the simplest and with the lowest requirements in terms of information exchange. The approach proposed in the previous paragraphs has similarities with the one proposed in [31]. However, here we consider that the small cell UTs transmit more than one stream, and the type of architecture considered is quite different. As mentioned, we consider a hybrid analog-digital architecture in this work and in [31], a fully digital architecture was assumed.

1) FULLY COORDINATED

In the fully coordinated approach, the alignment direction $\mathbf{V}$ is generated at the BS, and the macro-cell performance is the best. To achieve the best performance, the alignment direction, where the inter-tier interference resides, must span a subspace orthogonal to the signal space of the macro-cell signal. Mathematically, this corresponds to setting the alignment direction as follows

$$\mathbf{V} = \text{null}(\mathbf{G}_{a,0}^H \mathbf{H}_{0,0} \mathbf{W}_{a,0}). \tag{24}$$

Equation (24) ensures that no attenuation occurs in the desired signal when the interference is removed. To compute $\mathbf{V}$, we must compute first or have knowledge of the analog precoder and equalizer of the macro-cell terminals. However, as the alignment direction must be fed back to the secondary system at each transmission time interval (TTI), the feedback requirements can be quite demanding, at $2R_0N_s$ reals per TTI.

2) STATIC

In the static method, the alignment direction is predefined and does not change throughout the communication process. The alignment direction needs to be shared just once, at the beginning of the interaction. This implies a reduction in the performance, but the feedback requirements are greatly reduced.

3) 2n-BIT COORDINATED

In [35], the authors propose a $2n$-bit coordinated method where it is possible to achieve a compromise between performance and feedback requirements, ranging from the static method ($n = 0$) to the fully coordinated method ($n = \infty$). In this method, the alignment direction is obtained as in the fully coordinated method. However, instead of feeding back real numbers, only a quantized version of the alignment direction matrix is fed back. This quantized version feeds back n bits from the real part and other n bits from the complex part. Hence the $2n$-bit name, where $n = 1, 2, 3$. The quantized alignment direction matrix is given by

$$\mathbf{V}_q = f_Q(Re\{(\mathbf{V})\}) + if_Q(Im\{(\mathbf{V})\}), \tag{25}$$

where $f_Q(.)$ denotes the quantization function, and $Re\{.\}$ and $Im\{.\}$ the real and complex parts of the alignment direction $\mathbf{V}$.

As seen in [35] for a flat fading Rayleigh channel without spatial correlation and with independent channel realizations, 1 bit for each real and complex part of the IA vector ($n = 1$) shows promising results for a minimum feedback requirement. For our specific case, the channel is correlated along the spatial dimension and not Rayleigh-distributed. It is a narrowband clustered channel as described in section II.C. However, as will be verified in the numerical results section, the performance of the 1-bit scheme is close to the full-coordinated approach.

IV. NUMERICAL RESULTS

In this section, we compare the performance results for different combinations of the previously described precoder and equalizer designs. Two scenarios are considered with the main parameters shown in Table 1, each with six different schemes, as seen in Table 2. The main difference between scenario 1 and 2 is that the number of transmitting data streams of the second is twice the first.

In all schemes, we used (12) to compute the digital part of the equalizers (either BS or CU). The first precoder/equalizer scheme corresponds to the case where both analog precoders and equalizers are randomly generated as in (7), and the static method for the digital small cells UT precoders (see Section III.C). With this scheme, the system has the minimum inter-system feedback requirements, since the alignment direction must be shared only once. In the second scheme, we replace the static IA vector for the coordinated vector, with 2 ($n = 1$) quantization bits. In the third scheme,

TABLE 2. Precoder/equalizer designs.

Scheme	Analog Precoder	Analog Equalizer Small/Macro Cell	Alignment Direction
1	Random	Random	Static
2	Random	Random	2 bit
3	Random	Algorithm 1	2 bit
4	Algorithm 1	Algorithm 1	2 bit
5	Algorithm 1	Algorithm 1	Full-Coordinated
6	Full Digital		

we replace the random analog equalizer at both the small cell BS and macro-cell APs by the proposed algorithm, described in section III (Algorithm 1). In this case, the BS and the CU must estimate a channel with higher dimension than the previous scenarios. In the fourth scheme, the random analog precoder is replaced by the proposed algorithm. In this case, the UTs need to know more information about the channel regarding the previous scenarios. In the fifth scheme, the static IA vector is replaced by the full coordinated approach, where the inter-tier exchange information is the highest. Finally, at the sixth scheme, a fully digital system is considered, i.e., one RF chain is assumed per antenna, and the IA vector is computed based on a full coordinated approach.

For the channel model, $N_{cl} = 8$ clusters are considered, all with the same average power and each with $N_{ray} = 3$ rays with Laplacian distributed azimuth/elevation angles of arrival/departure as in [20]. The angle spread for both the transmitter and receiver is 8°. Although we used this specific value, similar results are obtained for larger angle spreads. The carrier frequency is set to 28 GHz, and the antenna spacing elements assumed to be half-wavelength. All results were obtained by considering QPSK modulation. The performance metric considered is the BER, which is presented as a function of the E_b/N_0, with E_b denoting the average bit energy and N_0 denoting the one-sided noise power spectral density, given by $E_b/N_0 = 1/(2\sigma^2)$.

Let us start by analyzing scenario 1. In Fig. 5, we present the results for macro-cell while Fig. 6 shows the results for the small cell. From Fig. 5, we can see that the performance is the worst for the first scheme since the analog precoders and equalizer are randomly generated, and the alignment vector is static. These results are expected since the information about the channels at the terminals is quite small. We can observe that just by using a 2-bit quantization of the alignment vector, scheme 2, the performance improves 10.6 dB for a BER=10^{-3}. The results also show that by using the proposed analog equalizer, scheme 3, the performance improves 15.9 dB for the same BER and by further using the proposed precoder, scheme 4, the performance improves 11 dB for a BER=10^{-3}. By replacing the 2-bit approach

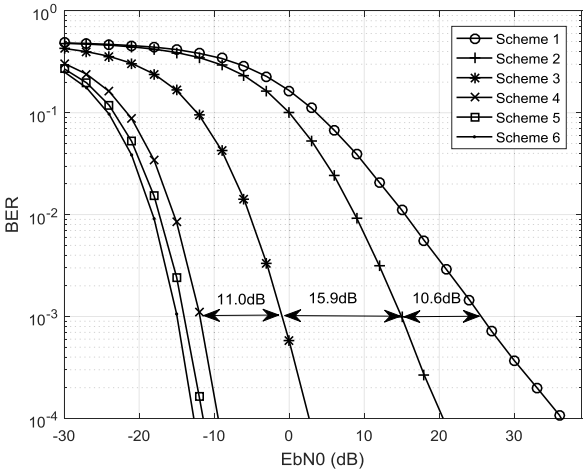

FIGURE 5. Macro-cell average BER for the first scenario.

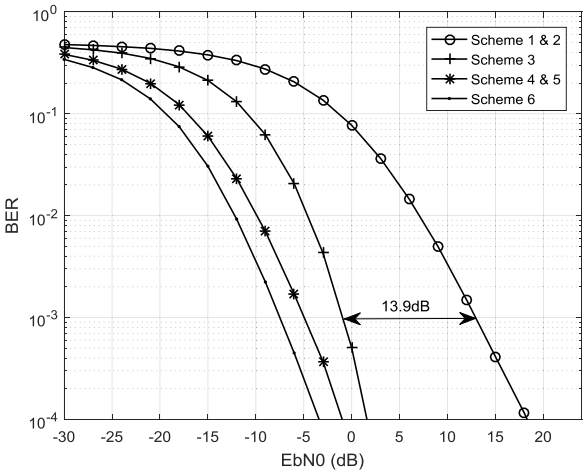

FIGURE 6. Small cell average BER for the first scenario.

(low overhead) with the full coordinated (high overhead), scheme 5, the improvement is small. We can also see that the performance of the proposed analog equalizer/precoder with a 2-bit quantization for the alignment (scheme 5) is very close the one achieved by the full coordinated approach, that can

be seen as the lower bound for the analog-digital approaches, indicating that the proposed hybrid scheme is quite efficient to remove the interference that the small cell UTs cause in the macro-cell BS using the degrees of freedom of the mmWave channel efficiently.

Fig. 6 (small cell results) shows that the performance of the scheme 1 and 2 is the same as in scheme 4 and 5. From Table 2, we can see that for these two pairs of schemes (scheme 1, 2 and scheme 4, 5), the analog equalizer and precoders are the same, only the alignment direction changes as a result of the independence between macro and small cell channels, which are used to compute the alignment direction and the precoders/equalizers, respectively. Similar to the macro case, scheme 5 has the best performance, which is identical to the scheme 4 as previously discussed. Again, the gap between the proposed hybrid scheme and the full digital approach is very small, which means that the proposed distributed scheme effective mitigates the multiuser and inter-tier interferences

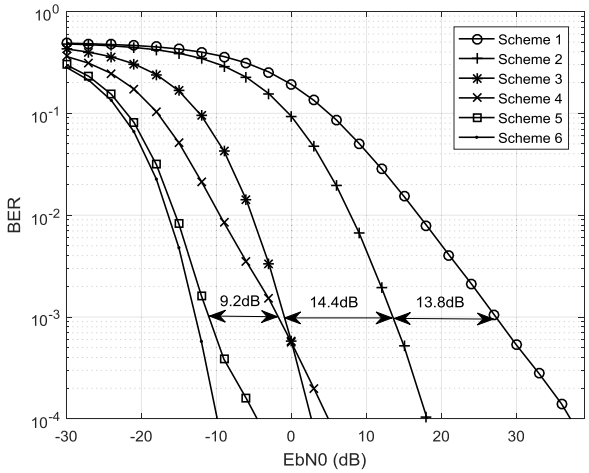

FIGURE 7. Macro-cell average BER for the second scenario.

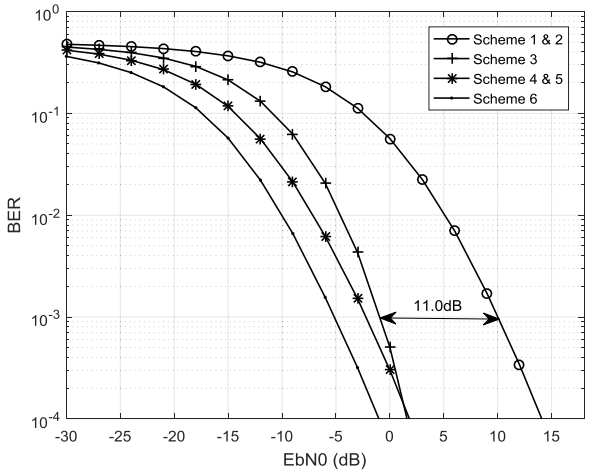

FIGURE 8. Small cell average BER for the second scenario.

The results for scenario 2 are depicted in Figs. 7 and 8 for macro and small cells, respectively. In this case, the number of transmitting data streams is twice the number of the first scenario, i.e., each UT transmits 2 data symbols in parallel. From these figures, we basically can note conclusions similar to scenario 1. From Fig. 7 (macro-cell results), it can be seen that by replacing the 2-bit quantization approach (scheme 4) with the full coordinated approach (scheme 5), the improvement is more significant than in the scenario 1, i.e., the gap between these two schemes is larger than in the first scenario. Therefore, scenario 2 requires more bits to approach the full coordinated approach and hence a higher overhead because now the level of interference is higher since the intra-tier interference is composed of the intersymbol and multi-user interference, contrary to scenario 1 which has only multi-user interference.

V. CONCLUSIONS

In this paper, we proposed low-feedback overhead hybrid analog-digital precoder and equalizer schemes for uplink of massive MIMO mmWave HetNets systems. The hybrid processing is performed in a distributed fashion at the small cells, where the analog part is performed at the small cell base stations or APs and the digital part at the CU for joint processing to efficiently remove the inter/intra tier interferences. To optimize the analog part of the hybrid equalizer and the precoders (used at the user terminals), we minimized the distance between the hybrid and the fully digital approaches. In the optimization problem, we imposed constraints of the analog part and the constraints inherent to distributed nature of the APs. To cancel the inter-tier interference, the digital part of the precoders employed at the small cell user terminals was designed in such a way that this interference resides in a low dimension subspace at the macro BS.

The results showed that the performance of the proposed hybrid analog-digital precoder/equalizer schemes is quite close to the fully digital counterpart. Furthermore, the results also showed that 2 bits of inter-tier information exchange are enough for most scenarios to efficiently align the interference with a good overall network performance. Therefore, the proposed hybrid scheme is quite efficient to remove both inter- and intra-tier interferences with very low network overhead.

REFERENCES

[1] J. Hoadley and P. Maveddat, "Enabling small cell deployment with HetNet," *IEEE Wireless Commun.*, vol. 19, no. 2, pp. 4–5, Apr. 2012.
[2] T. Nakamura *et al.*, "Trends in small cell enhancements in LTE advanced," *IEEE Commun. Mag.*, vol. 51, no. 2, pp. 98–105, Feb. 2013.
[3] A. Gupta and R. K. Jha, "A survey of 5G network: Architecture and emerging technologies," *IEEE Access*, vol. 3, pp. 1206–1232, Aug. 2015.
[4] F. Boccardi, R. W. Heath, Jr., A. Lozano, T. L. Marzetta, and P. Popovski, "Five disruptive technology directions for 5G," *IEEE Commun. Mag.*, vol. 52, no. 2, pp. 74–80, Feb. 2014.
[5] S. Rangan, T. S. Rappaport, and E. Erkip, "Millimeter-wave cellular wireless networks: Potentials and challenges," *Proc. IEEE*, vol. 102, no. 3, pp. 366–385, Mar. 2014.
[6] T. E. Bogale and L. B. Le, "Massive MIMO and mmWave for 5G wireless HetNet: Potential benefits and challenges," *IEEE Veh. Technol. Mag.*, vol. 11, no. 1, pp. 64–75, Mar. 2016.

[7] T. S. Rappaport, F. Gutierrez, E. Ben-Dor, J. N. Murdock, Y. Qiao, and J. I. Tamir, "Broadband millimeter-wave propagation measurements and models using adaptive-beam antennas for outdoor urban cellular communications," *IEEE Trans. Antennas Propag.*, vol. 61, no. 4, pp. 1850–1859, Apr. 2013.
[8] T. S. Rappaport, G. R. Maccartney, M. K. Samimi, and S. Sun, "Wideband millimeter-wave propagation measurements and channel models for future wireless communication system design," *IEEE Trans. Commun.*, vol. 63, no. 9, pp. 3029–3056, Sep. 2015.
[9] A. Alkhateeb, J. Mo, N. Gonzalez-Prelcic, and R. W. Heath, Jr., "MIMO precoding and combining solutions for millimeter-wave systems," *IEEE Commun. Mag.*, vol. 52, no. 12, pp. 122–131, Dec. 2014.
[10] F. Rusek *et al.*, "Scaling up MIMO: Opportunities and challenges with very large arrays," *IEEE Signal Process. Mag.*, vol. 30, no. 1, pp. 40–60, Jan. 2013.
[11] E. G. Larsson, O. Edfors, F. Tufvesson, and T. L. Marzetta, "Massive MIMO for next generation wireless systems," *IEEE Commun. Mag.*, vol. 52, no. 2, pp. 186–195, Feb. 2014.
[12] K. Zheng, L. Zhao, J. Mei, B. Shao, W. Xiang, and L. Hanzo, "Survey of large-scale MIMO systems," *IEEE Commun. Surveys Tuts.*, vol. 17, no. 3, pp. 1738–1760, 3rd Quart., 2015.
[13] A. Lee Swindlehurst, E. Ayanoglu, P. Heydari, and F. Capolino, "Millimeter-wave massive MIMO: The next wireless revolution?" *IEEE Commun. Mag.*, vol. 52, no. 9, pp. 52–62, Sep. 2014.
[14] T. S. Rappaport *et al.*, *Millimeter Wave Wireless Communications*, Englewood Cliffs, NJ, USA: Prentice-Hall, 2014.
[15] T. S. Rappaport, J. N. Murdock, and F. Gutierrez, "State of the art in 60-GHz integrated circuits and systems for wireless communications," *Proc. IEEE*, vol. 99, no. 8, pp. 1390–1436, Aug. 2011.
[16] A. Alkhateeb, O. El Ayach, G. Leus, and R. W. Heath, Jr., "Channel estimation and hybrid precoding for millimeter wave cellular systems," *IEEE J. Sel. Topics Signal Process.*, vol. 8, no. 5, pp. 831–846, Oct. 2014.
[17] O. El Ayach, S. Rajagopal, S. Abu-Surra, Z. Pi, and R. W. Heath, Jr., "Spatially sparse precoding in millimeter wave MIMO systems," *IEEE Trans. Wireless Commun.*, vol. 13, no. 3, pp. 1499–1513, Mar. 2014.
[18] J. Li, L. Xiao, X. Xu, and S. Zhou, "Robust and low complexity hybrid beamforming for uplink multiuser mmWave MIMO systems," *IEEE Commun. Lett.*, vol. 20, no. 6, pp. 1140–1143, Jun. 2016.
[19] A. Alkhateeb, G. Leus, and R. W. Heath, Jr., "Limited feedback hybrid precoding for multi-user millimeter wave systems," *IEEE Trans. Wireless Commun.*, vol. 14, no. 11, pp. 6481–6494, Nov. 2015.
[20] R. Magueta, D. Castanheira, A. Silva, R. Dinis, and A. Gameiro, "Hybrid iterative space-time equalization for multi-user mmW massive MIMO systems," *IEEE Trans. Commun*, vol. 65, no. 2, pp. 608–620, Feb. 2017.
[21] A. Alkhateeb and W. R. Heath, Jr., "Frequency selective hybrid precoding for limited feedback millimeter wave systems," *IEEE Trans. Commun.*, vol. 64, no. 5, pp. 1801–1818, May 2016.
[22] G. Wang, J. Sun, and G. Ascheid, "Hybrid beamforming with time delay compensation for millimeter wave MIMO frequency selective channels," in *Proc. IEEE Veh. Technol. Conf. (VTC Spring)*, May 2016, pp. 1–6.
[23] R. Rajashekar and L. Hanzo, "Iterative matrix decomposition aided block diagonalization for mm-wave multiuser MIMO systems," *IEEE Trans. Wireless Commun.*, vol. 16, no. 3, pp. 1372–1384, Mar. 2017.
[24] W. Ni, X. Dong, and W.-S. Lu, "Near-optimal hybrid processing for massive MIMO systems via matrix decomposition," *IEEE Trans. Signal Process.*, vol. 65, no. 15, pp. 3922–3933, Aug. 2017.
[25] Z. Wang, M. Li, X. Tian, and Q. Liu, "Iterative hybrid precoder and combiner design for mmWave multiuser MIMO systems," *IEEE Commun. Lett.*, vol. 21, no. 7, pp. 1581–1584, Jul. 2017.
[26] T. Nakamura *et al.*, "Trends in small cell enhancements in LTE advanced," *IEEE Commun. Mag.*, vol. 51, no. 2, pp. 98–105, Feb. 2013.
[27] V. R. Cadambe and S. A. Jafar, "Interference alignment and degrees of freedom of the K-user interference channel," *IEEE Trans. Inf. Theory*, vol. 54, no. 8, pp. 3425–3441, Aug. 2008.
[28] D. Castanheira, A. Silva, and A. Gameiro, "Retrospective interference alignment: Degrees of freedom scaling with distributed transmitters," *IEEE Trans. Inf. Theory*, vol. 63, no. 3, pp. 1721–1730, Mar. 2017.
[29] M. Maso, M. Debbah, and L. Vangelista, "A distributed approach to interference alignment in OFDM-based two-tiered networks," *IEEE Trans. Veh. Technol.*, vol. 62, no. 5, pp. 1935–1949, Jun. 2013.
[30] S. K. Sharma, S. Chatzinotas, and B. Ottersten, "Interference alignment for spectral coexistence of heterogeneous networks," *EURASIP J. Wireless Commun. Netw.*, vol. 2013, no. 1, p. 46, Dec. 2013.
[31] D. Castanheira, A. Silva, and A. Gameiro, "Set optimization for efficient interference alignment in heterogeneous networks," *IEEE Trans. Wireless Commun.*, vol. 13, no. 10, pp. 5648–5660, Oct. 2014.
[32] D. Castanheira, A. Silva, R. Dinis, and A. Gameiro, "Efficient transmitter and receiver designs for SC-FDMA based heterogeneous networks," *IEEE Trans. Commun.*, vol. 63, no. 7, pp. 2500–2510, Jul. 2015.
[33] N. Benvenuto, R. Dinis, D. Falconer, and S. Tomasin, "Single carrier modulation with nonlinear frequency domain equalization: An idea whose time has come—Again," *Proc. IEEE*, vol. 98, no. 1, pp. 69–96, Jan. 2010.
[34] A. Thampi, S. C. Liew, S. Armour, Z. Fan, L. You, and D. Kaleshi, "Physical-layer network coding in two-way heterogeneous cellular networks with power imbalance," *IEEE Trans. Veh. Technol.*, vol. 65, no. 11, pp. 9072–9084, Nov. 2016.
[35] S. S. Ali, D. Castanheira, A. Silva, and A. Gameiro, "Joint signal alignment precoding and physical network coding for heterogeneous networks," *Phys. Commun.*, vol. 23, no. 1, pp. 125–133, Jun. 2017.
[36] G. Xu, C.-H. Lin, W. Ma, S. Chen, and C.-Y. Chi, "Outage constrained robust hybrid coordinated beamforming for massive MIMO enabled heterogeneous cellular networks," *IEEE Access*, vol. 5, pp. 13601–13616, Mar. 2017.
[37] T. Bai and R. W. Heath, Jr., "Coverage and rate analysis for millimeter-wave cellular networks," *IEEE Trans. Wireless Commun.*, vol. 14, no. 2, pp. 1100–1114, Feb. 2015.
[38] T. S. Rappaport *et al.*, "Millimeter wave mobile communications for 5G cellular: It will work!" *IEEE Access*, vol. 1, pp. 335–349, May 2013.

DANIEL CASTANHEIRA received the Licenciatura (ISCED level 5) and Ph.D. degrees in electronics and telecommunications from the University of Aveiro in 2007 and 2012, respectively. In 2011, he was with the Departamento de Eletrónica, Telecomunicações e Informática, Aveiro University, as an Assistant Professor. He has been involved in several national and European projects, namely RETIOT, SWING2, PURE-5GNET, HETCOP, COPWIN, and PHOTON within the FCT Portuguese National Scientific Foundation, and CODIV, FUTON, and QOSMOS with the FP7 ICT. He is currently an Auxiliary Researcher with the Instituto the Telecomunicações, University of Aveiro, Aveiro, Portugal. His research interests lie in signal processing techniques for digital communications, with emphasis for physical layer issues, including channel coding, precoding/equalization, and interference cancelation.

PEDRO LOPES is currently pursuing the M.Sc. degree in electronics and telecommunications engineering with the University of Aveiro, Portugal. At the university, he is involved in the M.Sc. dissertation Massive MIMO processing techniques for Heterogeneous LTE-Advanced/5G mobile systems. In 2016, he enrolled for a year in an undergraduate research scholarship in the development of innovative UWB antennas with the Institute of Telecommunications, Aveiro, Portugal. He is also an Intern with ENEIDA.IO, Coimbra, Portugal, where he is in charge of enhancing radio communications. His research interests include antennas and wireless communications, with a special focus on hybrid architectures and multiple antennas techniques.

ADÃO SILVA received the M.Sc. and Ph.D. degrees in electronics and telecommunications from the University of Aveiro in 2002 and 2007, respectively. He is currently an Assistant Professor with the Department of Electronics, Telecommunications and Informatics, University of Aveiro, and a Senior Researcher with the Instituto de Telecomunicações. He has been participating in several national and European projects, namely the ASILUM, MATRICE, 4MORE within the ICT programme, and the FUTON and CODIV projects with the FP7 ICT. He has led several research projects, in the broadband wireless communications area, at the national level. His interests include multiuser MIMO, multicarrier-based systems, cooperative networks, precoding, multiuser detection, and massive MIMO and millimeter wave communications. He acted as a member of the TPC of several international conferences.

ATÍLIO GAMEIRO received the Licenciatura and Ph.D. degrees from the University of Aveiro in 1985 and 1993, respectively. His industrial experience includes a period of one year at BT Labs and one year at NKT Elektronik. He is currently an Associate Professor with the Department of Electronics and Telecommunications, University of Aveiro, and a Researcher with the Instituto de Telecomunicações, Pólo de Aveiro, where he is also the Head of the group. He has been involved and has led IT or University of Aveiro participation on more than 20 national and European projects. He has published over 200 technical papers in international journals and conferences. His main interests lie in signal processing techniques for digital communications and communication protocols, and within this research line, he has done work for optical and mobile communications, either at the theoretical and experimental level. His current research activities involve space-time-frequency algorithms for the broadband wireless systems and cross-layer design.